Magnetization Reversal of Individual Co Nanoislands

S. Ouazi, S. Wedekind, G. Rodary,* H. Oka, D. Sander, and J. Kirschner

Max-Planck-Institut für Mikrostrukturphysik, Weinberg 2, D-06120 Halle/Saale, Germany
(Received 31 August 2011; published 9 March 2012)

We investigate the magnetization reversal of individual Co islands on Cu(111) in the size range of $N = 700$ to $18\,000$ atoms by spin-polarized scanning tunneling microscopy at 8 K. The switching field H_{sw} changes with island size in a nonmonotonic manner: it increases with island size and reaches a maximum value of 2.4 T at $N = 5500$ atoms, and it decreases for larger islands. We extract the energy barrier for magnetization reversal as a function of island size. The maximum H_{sw} corresponds to an energy barrier of 1 eV. Our results elucidate a crossover of the magnetization reversal from an exchange-spring behavior to domain wall formation with increasing size at around 7500 atoms.

An outstanding challenge in nanomagnetism is the quantitative understanding of magnetization reversal of nanoparticles [1], which has also profound implications for magnetic recording media [2,3]. In some cases, the exchange interaction leads to a parallel alignment of all magnetic moments, and the reversal can be described by a coherent rotation of a so-called macrospin. The venerable Stoner-Wohlfarth model of magnetization reversal describes this process [4], and it has been applied successfully to numerous real-world nanostructures [5–7]. An alternative reversal mechanism is the nucleation of magnetic domains, and their growth upon magnetization reversal. *A priori* it is not clear which reversal mechanism applies for a given nanostructure, and other reversal processes are also conceivable [8,9]. A key factor in the understanding of magnetization reversal is the energy barrier ΔE, which needs to be overcome to toggle the system between two stable magnetization states. Measurements of the magnetic switching field H_{sw} and the extraction of ΔE for nanoparticles of different size help to identify the reversal process. However, the experimental data base on these properties of individual well-characterized nanostructures is very scarce.

In this Letter, we report the size dependence of H_{sw} for individual nanoislands, and this allows us to characterize a size-driven crossover between two different reversal regimes on the nanometer scale. We exploit the high spatial resolution and the magnetic sensitivity of spin-polarized scanning tunneling spectroscopy (spin-STS) to measure H_{sw} of individual, well-characterized two atoms thick Co nanoislands. The spatial resolution of STM measurements allows us to select individual islands with similar shape, but different size. We find that H_{sw} increases with the island size up to 5500 atoms, where $\mu_0 H_{sw} = 2.4$ T at 8 K. H_{sw} declines for larger islands. Although the general trend of the dependence of H_{sw} on island size is expected [10], its quantitative analysis leads to a surprising result. Small Co islands ($\simeq 1000$ atoms) switch too easily as compared to the expectations based on the

Stoner-Wohlfarth model. Our quantitative analysis suggests that the Co islands are magnetically inhomogeneous. We propose that the outer rim of the Co island is magnetically soft, whereas the center region is magnetically hard. Both phases interact by magnetic exchange coupling. Thus, Co islands may be regarded as a single element exchange-spring nanomagnet [11]. For larger islands, we propose that the magnetization reversal occurs by domain nucleation and growth.

The STM and spin-STS experiments have been performed at 8 K in an ultrahigh-vacuum chamber with a base pressure in the low 10^{-11} mbar range. The Cu(111) substrate has been cleaned prior to Co deposition by cycles of ion bombardment (Ar$^+$, 1 keV, 1 μA, 600 s) and subsequent annealing at 700 K for 10 minutes. To obtain magnetic contrast, W tips have been electrochemically etched, subsequently flashed to 2400 K under ultrahigh vacuum conditions, and covered with a magnetic material (Cr and/or Co), as described in [12]. The deposition of a submonolayer amount of Co atoms at room temperature leads to the formation of double layer high islands which are often of triangular shape [13]. Figure 1 shows a constant-current STM image of several typical Co islands on Cu(111). A quantitative analysis of the STM images provides the area $\mathcal{A}$ of these islands in nm^2. From $\mathcal{A}$ in nm^2 we calculate the island size in number of atoms $N = \mathcal{A}/0.028$. The relative error of $\mathcal{A}$ is smaller than 5%. Figure 1 shows that the shape of the selected islands A to D is similar, while the size varies from $N = 1600$ to $13\,100$ atoms. The different orientations of islands A and C versus B and D with respect to the underlying substrate correspond to the faulted and unfaulted layer stackings, respectively, as defined in [14]. The STM is at the center of a superconducting magnet, which produces a magnetic field of up to ± 7.0 T perpendicular to the sample plane. We measure the field-dependence of the differential conductance dI/dV, to access the magnetization state of the islands [12,15]. For one specific field value, we obtain a dI/dV spectrum in 100 seconds, which marks the
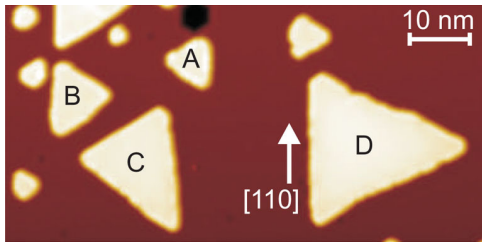
FIG. 1 (color).   Constant-current mode measurement of double
layer high (0.4 nm) Co islands on Cu(111) ($I = 1$ nA, $V =
-0.27$ V, $T = 8$ K). The labeled islands have been selected
for the spin-STS measurements, and these labels are used in
Figs. 1–4.

characteristic time of our measurements. Figure 2 presents
the magnetic hysteresis curves of islands A to D. In total we
investigated the magnetic properties of 54 selected islands.

Figure 2 shows the field dependence of the differential
conductance dI/dV measured at the center of the Co
islands A to D of Fig. 1. The same tip has been used for
these measurements, as confirmed by the spectroscopic
signature. For each field value, a complete spectrum
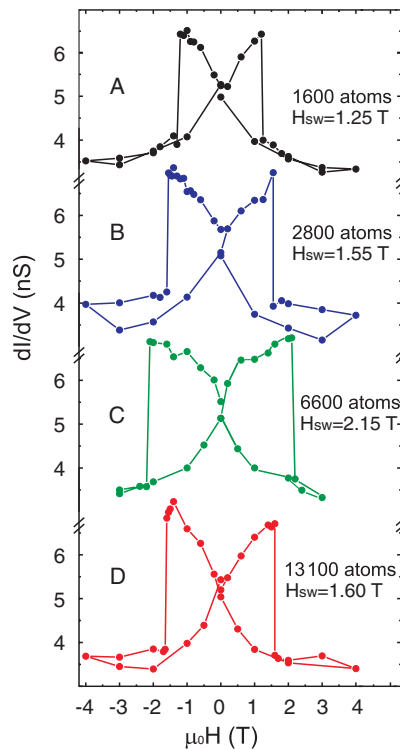$dI/dV(V)$ is measured, and the result for a gap voltage

of $V = -0.5$ V is plotted in Fig. 2. Let us focus on the
hysteresis loop of island A. When the field is increased
from 0 to $+1.2$ T, the dI/dV signal continuously in-
creases. Between 1.2 and 1.3 T, the curve shows a drop
by 2.5 nS and then gradually approaches 3.5 nS. This drop
reveals the magnetization reversal of the Co island [12,15].
We get $\mu_0 H_{sw} = 1.25 \pm 0.05$ T for island A. The value of
H_{sw} for one specific island is very reproducible, within
± 0.05 T for repeated measurements. When the field is
cycled back to zero, the dI/dV signal reverts to its initial
value. In connection with a negative field cycle, we obtain
a symmetric curve within experimental error.

Symmetric hysteresis curves are commonly found for
spin-polarized tunneling between two ferromagnetic elec-
trodes (here: magnetic tip and Co island). The symmetry
reveals that both electrodes change their magnetization
direction with the applied magnetic field. A typical butter-
fly shaped curve results, as has been first reported for
magnetic tunnel junctions [16] and later in spin-STS mea-
surements [12,15]. The hysteresis loops in Fig. 2 present all
a similar butterfly shape revealing that the tip response to
the magnetic field is the same. On the contrary, the position
of the dI/dV signal drop differs for the different islands.
For islands A to C the switching field increases from 1.25
to 2.15 T, while the island size grows from 1600 to
6600 atoms. The largest island D has a smaller switching
field of 1.6 T, as compared to island C.

Figure 3 summarizes our measurements of the switching
field H_{sw} for different island sizes N. A nonmonotonic
dependence of H_{sw} on N is apparent. H_{sw} increases from
0.25 to 2.5 T for an increasing size N from $N = 700$ to
6000 atoms, and it decreases for larger islands. To gain
further insights into the physics of the reversal mechanism
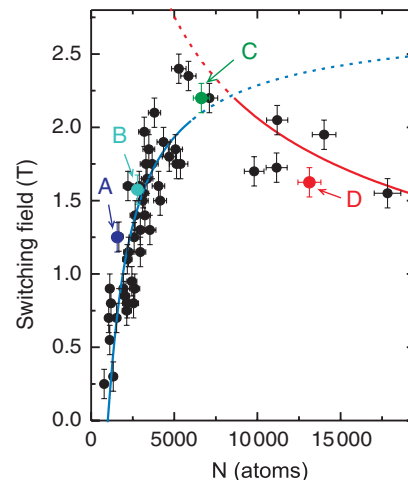we derive the energy barrier ΔE from H_{sw} in the following

FIG. 2 (color).   Hysteresis curves of the differential conduc-
tance dI/dV measured at the center of islands A to D. The
magnetic field is applied perpendicularly to the substrate surface.
Note, that due to the reorientation of the magnetization of the
neighboring islands and of the tip, magnetic stray fields vary
during a field scan. We estimate these field variations smaller
than 0.1 T. ($V = -0.5$ V and $T = 8$ K).

FIG. 3 (color).   Switching fields of 54 individual Co islands of
different size. Data points of islands A to D from Fig. 1 are
indicated. The red and blue lines are calculated from two differ-
ent reversal mechanism, as described in the text. They do not
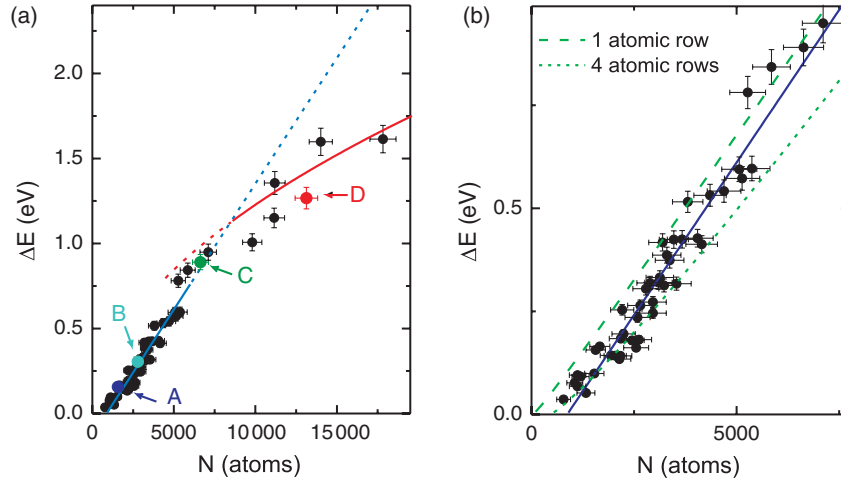represent fits through the data points.

FIG. 4 (color). Island size dependence of the energy barrier ΔE. (a) The blue curve is a linear fit $\Delta E_{\text{lin}}(N) = K(N - N_0)$, as described in the text. The red curve shows the calculated energy barrier for domain wall formation $\Delta E_{\text{dw}}(N) = 4\sigma\sqrt{AK}$. The labels identify the data for the islands of Fig. 1. (b) The blue line is the same as in (a). The function $K(N - N_{\text{rim}})$ is plotted for different rim widths of 1 and 4 atomic rows, respectively, with dashed and dotted green lines.

way. If a magnetic field H is applied opposite to the magnetization direction, the apparent barrier is given by $E(H) = \Delta E(1 - H\frac{N\mu}{2\Delta E})^2$ [1] where μ is the magnetic moment per atom. Thermal fluctuations help the system to cross this barrier, as pointed out by Néel and Brown [17]. At a temperature T, the relation between the switching field and the energy barrier is:

$$H_{\text{sw}} = \frac{2\Delta E}{N\mu}\left[1 - \left(\frac{k_B T}{\Delta E}\ln\frac{t_{\text{meas}}}{\tau_0}\right)^{1/2}\right]. \quad (1)$$

We use $\tau_0 = 10^{-10}$ s [8] and $t_{\text{meas}} = 100$ s, which reflects the time of one spectroscopy scan.

Figure 4(a) presents the dependence of the energy barrier ΔE on island size N. Figure 4(b) shows a zoom-in for smaller N. The data points cluster around a linear ΔE vs N dependence up to $N \approx 7500$ atoms. An extrapolation of ΔE to zero leads to an offset N_0. Data points for $N > 7500$ fall below this linear extrapolation. The Stoner-Wohlfarth model proposes that the energy barrier corresponds to the total anisotropy of the island, $\Delta E = KN$, where the anisotropy and island size are given by K and N, respectively. In view of this, the offset N_0 is a remarkable unexpected result. The blue line is a linear fit through the data points for $N < 7500$, with the relation $\Delta E_{\text{lin}}(N) = K(N - N_0)$. The slope gives $K = 0.148 \pm 0.005$ meV/atom, and we observe an offset of $N_0 = 870 \pm 150$ atoms. It implies that only a reduced number of atoms $(N - N_0)$ contributes to the magnetic anisotropy K. What is the physical origin of this offset?

The high spatial resolution of differential conductance measurements by STM have revealed that the electronic structure within a single Co nanoisland varies dramatically upon approaching the rim region. Whereas almost spatially constant spectroscopy is observed in the center region of

larger islands, spectral features change and new specific edge-related features appear near the edges [18–20]. Thus, we expect that these variations of the electronic structure do also impact the magnetic properties of the island, such as the magnetic anisotropy. We correlate the offset N_0 with the number of atoms N_{rim} in an effective rim relevant for the magnetic properties. To be more quantitative, we consider in Fig. 4(b) the size dependence of N_{rim}, for two different rim widths of one and four atomic rows. The corresponding energy barrier is compared with the experimental data points which are bounded by these two extreme widths. We conclude that the effective rim for the magnetic properties is between one and four atomic rows wide [21]. From close inspection of Fig. 4(b), we may speculate that this width varies with island size, and it appears to be larger for smaller islands.

Our analysis leads us to propose that we may regard the Co islands as a one-element exchange-spring system [11]. The rim contributes to the magnetization, but not to the magnetic anisotropy. We propose that Co atoms near the rim are magnetically soft; i.e., they show a negligible effective magnetic anisotropy as compared to the inner part of the Co island. The magnetocrystalline anisotropy K_{mc} of the inner part is given by K, corrected for the dipolar anisotropy (-0.11 meV/atom). We find for the inner part $K_{\text{mc}} = 0.25$ meV/atom or 3.4 MJ/m³. This simplified distinction between two magnetic phases appears to be a valid first step to clarify the most relevant features for the magnetization reversal. The magnitude of N_0 suggests that the width of the magnetically soft area corresponds roughly to the extension of the so-called electronic rim state [18]. Whether this is a coincidence or a decisive aspect of the peculiar magnetic anisotropy of this system remains a topic of future in depth theoretical work. In view of numerous studies on extended monolayers, it is

physically sound and well justified to consider a significant correlation between structural and electronic relaxation and magnetic anisotropy also near the boundaries of nanostructures [22]. These relaxation effects extend over several atomic distances towards the inner part of the nanostructure. It was already known that edge atoms can have a magnetic behavior quite different from atoms inside a structure. However, they usually display a higher magnetic anisotropy, as expected from their lower coordination [23]. Our present work shows that coordination effects are comparably less important. Rather, the magnetic properties of Co islands on Cu(111) appear to be affected by the variation of the electronic properties near the rim region. Within our resolution, we did not observe an influence of the stacking on the energy barrier.

For $N \gtrsim 7000$ atoms, Fig. 4 shows that the energy barrier ΔE deviates from the linear fit to smaller values. This deviation marks the crossover to another magnetization reversal mechanism. Here, we compare ΔE to the energy cost for domain wall formation $\Delta E_{dw}(N) = 4\sigma\sqrt{AK}$ [1]. σ is the area of the domain wall, and it is given by the island morphology. We calculated it from a vertical cross-section $\sigma = d \times \ell$ with $d = 2$ atoms and ℓ the geometric height of the inner part, given by the STM measurements for each island. Thus ℓ is defined as the maximal length of the domain wall. $A = 27.1$ meV/atom is the exchange constant and $K = 0.148 \pm 0.005$ meV/atom is the anisotropy energy density. We note that we never observed domains on an individual island. This does not come as a surprise, as the reversal process is expected to occur on a much shorter time scale as compared to the speed of our measurements. The red line in Fig. 4(a) shows the curve of $\Delta E_{dw}(N)$. The agreement between the measured and calculated energy barrier is remarkable. Not only the trend of ΔE but even the numerical values are reproduced. The scenario of domain wall formation as the magnetization reversal mechanism in larger islands is reasonable. We note that for the smallest islands we have $\Delta E_{lin} < \Delta E_{dw}$ whereas for $N \gtrsim 8000$ atoms $\Delta E_{lin} > \Delta E_{dw}$ and therefore the system chooses the most energetically favorable reversal mechanism. We calculate the switching fields corresponding to these results for ΔE_{lin} and ΔE_{dw}, and we present the results as blue and red curves, respectively, in Fig. 3. The curves describe the experimental data on H_{sw} very well, and this provides additional support for the reversal mechanism discussed here.

In conclusion, using the spatial resolution and the magnetic sensitivity of in-field spin-polarized scanning tunneling spectroscopy measurements, we investigated the size dependence of the switching field of Co islands on Cu(111). We identify two regimes for the size dependence of H_{sw} which are ascribed to two magnetization reversal mechanisms. In smaller islands ($N < 7000$ atoms), the switching field increases with island size, and

the magnetization reversal shows the characteristics of an exchange-spring magnet. A quantitative analysis suggests that the island rim is magnetically soft. The switching field decreases for larger islands. We ascribe this to a crossover to a magnetization reversal via domain wall formation. It remains a topic of future experimental and theoretical research to establish the electronic origin of the link between structural relaxation, mesoscopic misfit [24], and magnetic anisotropy of individual nanostructures. Such studies could elucidate if possible spatial variations of A or μ are also significant in view of the reversal process.

*Now at: Laboratoire de Photonique et de Nanostructures/ CNRS, Route de Nozay, 91460 Marcoussis, France

[1] R. O'Handley, *Modern Magnetic Materials: Principles and Applications* (Wiley, New York, 2000).

[2] D. Weller and A. Moser, IEEE Trans. Magn. **35**, 4423 (1999).

[3] A. Berger, N. Supper, Y. Ikeda, B. Lengsfield, A. Moser, and E. E. Fullerton, Appl. Phys. Lett. **93**, 122502 (2008).

[4] E. Stoner and E. Wohlfarth, Phil. Trans. R. Soc. A **240**, 599 (1948).

[5] W. Wernsdorfer, E. B. Orozco, K. Hasselbach, A. Benoit, B. Barbara, N. Demoncy, A. Loiseau, H. Pascard, and D. Mailly, Phys. Rev. Lett. **78**, 1791 (1997).

[6] W. Wernsdorfer, E. Bonet Orozco, K. Hasselbach, A. Benoit, D. Mailly, O. Kubo, H. Nakano, and B. Barbara, Phys. Rev. Lett. **79**, 4014 (1997).

[7] A. Lehnert, P. Buluschek, N. Weiss, J. Giesecke, M. Treier, S. Rusponi, and H. Brune, Rev. Sci. Instrum. **80**, 023902 (2009).

[8] W. Wernsdorfer, Adv. Chem. Phys. **118**, 99 (2001).

[9] D. A. Garanin and H. Kachkachi, Phys. Rev. B **80**, 014420 (2009).

[10] E. Kneller and F. Luborsky, J. Appl. Phys. **34**, 656 (1963).

[11] H. Zeng, J. Li, J. Liu, Z. Wang, and S. Sun, Nature (London) **420**, 395 (2002).

[12] G. Rodary, S. Wedekind, H. Oka, D. Sander, and J. Kirschner, Appl. Phys. Lett. **95**, 152513 (2009).

[13] J. de la Figuera, J. E. Prieto, C. Ocal, and R. Miranda, Phys. Rev. B **47**, 13043 (1993).

[14] N. N. Negulyaev, V. S. Stepanyuk, P. Bruno, L. Diekhöner, P. Wahl, and K. Kern, Phys. Rev. B **77**, 125437 (2008).

[15] G. Rodary, S. Wedekind, D. Sander, and J. Kirschner, Jpn. J. Appl. Phys. **47**, 9013 (2008).

[16] J. S. Moodera, L. R. Kinder, T. M. Wong, and R. Meservey, Phys. Rev. Lett. **74**, 3273 (1995).

[17] W. F. Brown, Phys. Rev. **130**, 1677 (1963).

[18] O. Pietzsch, S. Okatov, A. Kubetzka, M. Bode, S. Heinze, A. Lichtenstein, and R. Wiesendanger, Phys. Rev. Lett. **96**, 237203 (2006).

PHYSICAL REVIEW LETTERS

[19] M. V. Rastei, B. Heinrich, L. Limot, P. A. Ignatiev, V. S. Stepanyuk, P. Bruno, and J. P. Bucher, Phys. Rev. Lett. **99**, 246102 (2007).

[20] H. Oka, P. A. Ignatiev, S. Wedekind, G. Rodary, L. Niebergall, V. S. Stepanyuk, D. Sander, and J. Kirschner, Science **327**, 843 (2010).

[21] We considered for these two functions $K = 0.148$ meV/atom and used a square-root dependence of N_{rim} with the island size given by the island geometry.

[22] D. Sander, W. Pan, S. Ouazi, J. Kirschner, W. Meyer, M. Krause, S. Müller, L. Hammer, and K. Heinz, Phys. Rev. Lett. **93**, 247203 (2004).

[23] S. Rusponi, T. Cren, N. Weiss, M. Epple, P. Buluschek, L. Claude, and H. Brune, Nature Mater. **2**, 546 (2003).

[24] O. V. Lysenko, V. S. Stepanyuk, W. Hergert, and J. Kirschner, Phys. Rev. Lett. **89**, 126102 (2002).